PROCEEDINGS OF SCIENCE

Progress report on computing the disconnected QCD and the QCD plus QED hadronic contributions to the muon's anomalous magnetic moment

Alexei Bazavov,[a,b] **Christine Davies,**[c] **Carleton DeTar,**[d] **Aida El-Khadra,**[e] **Steven Gottlieb,**[f] **Dan Hatton,**[c] **Hwancheol Jeong,**[f] **Andreas Kronfeld,**[h] **Peter Lepage,**[i] **Craig McNeile,**[j,*] **Gaurav Ray,**[j] **James Simone**[h] **and Alejandro Vaquero**[d]

[a] *Department of Physics and Astronomy, Michigan State University, East Lansing, MI 48824, USA*
[b] *Department of Computational Mathematics, Science and Engineering, Michigan State University, East Lansing, MI 48824, USA*
[c] *SUPA, School of Physics and Astronomy, University of Glasgow, Glasgow, G12 8QQ, UK*
[d] *Department of Physics and Astronomy, University of Utah, Salt Lake City, UT 84112, USA*
[e] *Department of Physics, University of Illinois, Urbana, IL 61801, USA*
[f] *Department of Physics, Indiana University, Bloomington, Indiana, 47405, USA*
[h] *Fermi National Accelerator Laboratory, Batavia, IL 60510 USA*
[i] *Laboratory for Elementary-Particle Physics, Cornell University, Ithaca, NY 14853, USA*
[j] *Centre for Mathematical Sciences, University of Plymouth, UK*

E-mail: craig.mcneile@plymouth.ac.uk

Fermilab Lattice, HPQCD, and MILC Collaborations

We report progress on calculating the contribution to the anomalous magnetic moment of the muon from the disconnected hadronic diagrams with light and strange quarks and the valence QED contribution to the connected diagrams. The lattice QCD calculations use the highly-improved staggered quark (HISQ) formulation. The gauge configurations were generated by the MILC Collaboration with four flavors of HISQ sea quarks with physical sea-quark masses.

The 38th International Symposium on Lattice Field Theory, LATTICE2021 26th-30th July, 2021
Zoom/Gather@Massachusetts Institute of Technology

*Speaker

1. Introduction

The exciting recent results from the Fermilab Muon g-2 experiment for the muon anomalous magnetic moment [1], which are consistent with the previous result from the E821 experiment at BNL [2], motivates reducing the errors on lattice QCD calculations of the leading order hadronic vacuum polarization contribution to the muon anomalous magnetic moment $a_\mu^{\rm HVP,LO}$. There is a comprehensive recent review [3] of the theoretical calculations of $a_\mu^{\rm HVP,LO}$.

The latest result [4] from our program [5–9] of computing $a_\mu^{\rm HVP,LO}$is the value of the connected light quark contribution $a_\mu^{\rm HVP,LO}$with an error of 1.4%. Specifically, the final result for $10^{10} a_\mu^{HVP,LO} = 699(15)_{u,d}(1)_{s,c,b}$, included an estimate for the disconnected contribution $\Delta a_\mu^{\rho\omega}({\rm disc}) = -5(5) \times 10^{10}$ and residual QED corrections of $\Delta a_\mu^{\rho\omega}({\rm qed}) = 0(5) \times 10^{10}$. To reduce the final error to below ≈ 0.5 % we need to explicitly calculate the disconnected contributions and the QED corrections to $a_\mu^{\rm HVP,LO}$. In this paper, we report on the progress towards this goal.

There are other ongoing projects aimed at reducing the overall error on $a_\mu^{\rm HVP,LO}$within our collaboration, such as reducing the errors on the determination of the lattice spacing [10, 11], as well as reducing the error on the light quark connected contribution [12].

2. Overview of the analysis method

The leading-order contribution to the anomalous magnetic moment from the HVP is

$$a_\mu^{\rm HVP,LO} = 4\alpha^2 \int_0^\infty dq^2 f(q^2) \hat{\Pi}(q^2) \tag{1}$$

where $f(q^2)$ is a weighting factor [13]. $\hat{\Pi}(q^2)$ is the reduced vacuum polarization

$$\hat{\Pi}(q^2) = \frac{4\pi^2}{q^2} \int_0^\infty dt G(t) \left[q^2 t^2 - 4 \sin^2(\frac{qt}{2}) \right] \tag{2}$$

which can computed from the electromagnetic current correlator

$$G(t) = \frac{1}{3} \int d\mathbf{x} \sum_{f,i} q_f^2 Z_V^2 \langle V_i^f(\mathbf{x}, t) V_i^f(\mathbf{0}, 0) \rangle \tag{3}$$

where the sum is over flavors f with charges q_f for the vector current V_i^f. We use the kernel function method [14, 15]:

$$a_\mu^{\rm HVP,LO} = \sum_{t=0}^{\infty} w_t G(t) \tag{4}$$

to compute $a_\mu^{\rm HVP,LO}$, where w_t is a known weighting factor. The correlator $G(t)$ in Eq. 3 is very noisy at large t, so the fitted correlator is used after a time $t^\star$.

We use the HISQ action [16] for all quark propagators contributing to $G(t)$ and work on gluon field configurations that incorporate 2+1+1 flavors of sea quarks using the HISQ action [17, 18].

Ensemble	a fm	m_π MeV	L fm	Eigenmodes	N_{meas}
Very coarse	0.15	134.7	4.8	300	1692
Coarse	0.12	134.9	5.8	-	787
Fine	0.09	128.3	5.8	1000	271

Table 1: HISQ ensembles used in the disconnected analysis

3. Computatation of the disconnected contribution

The disconnected contribution requires the non-perturbative calculation of the quark-line disconnected correlation of vector currents. For the disconnected contribution we use the taste-singlet vector operator. The Z_V renormalization factor used was computed using the RI-SMOM scheme [19]. We use stochastic random sources to compute the required loops with a variety of variance reduction techniques [20, 21].

The SU(3) structure of the vector current requires that the loop for the operator

$$V_j^{ls} = \frac{1}{3}(V_j^l - V_j^s) \tag{5}$$

be computed for the light quark (l) and strange quark (s). This object can be efficiently calculated using a technique developed by the ETM collaboration [22], which was used in the calculation of the mass of the η' [23] and ω meson [24], as well as calculations of flavour singlet nucleon matrix elements [25]. This method has also been proposed and further developed by Giusti et al. [26].

The measurement in QCD of the loop of the operator in Eq. 5 requires the computation of

$$L(t)^{ls} = \left\langle \mathrm{Tr}\left(\gamma_\mu \frac{1}{\not{D} + m_l} - \gamma_\mu \frac{1}{\not{D} + m_s} \right) \right\rangle \tag{6}$$

where $\not{D}$ is the massless HISQ Dirac operator.

The difference in Eq. 6 can be trivially written down as:

$$L(t)^{ls} = \left\langle \mathrm{Tr}\left(\gamma_\mu \frac{(m_s - m_l)}{(\not{D} + m_l)(\not{D} + m_s)} \right) \right\rangle \tag{7}$$

The right hand side of Eq. 7 can be computed using noise sources. In Ref. [22] ETM have argued that Eq. 7 has a smaller variance than Eq. 6. We have computed $a_\mu^{\mathrm{HVP(LO),DISC}}$ for the light and strange quarks. The ensembles used to compute disconnected correlators are listed in Table 1. To remove potential subjective bias, we do a "blinded analysis." The correlators are multiplied by a random blinding factor [27]. For the fine ensemble, we used Eq. 7 with the truncated solver method [28, 29] combined with deflation of 1000 low-modes [30].

We broadly follow the analysis method described in Ref. [6]. We fit the correlators to a model of the difference of correlators between flavour singlet and non-singlet mesons and replace the correlator in Eq. 4 at time larger than $t^\star$ with the fitted correlator.

$$G(t) = \sum_{i=1}^{N} [b_i^2 e^{-E_{b_i} t} - a_i^2 e^{-E_{a_i} t} + (-1)^t \left(c_i^2 e^{-E_{c_i} t} - d_i^2 e^{-E_{d_i} t} \right)] \tag{8}$$

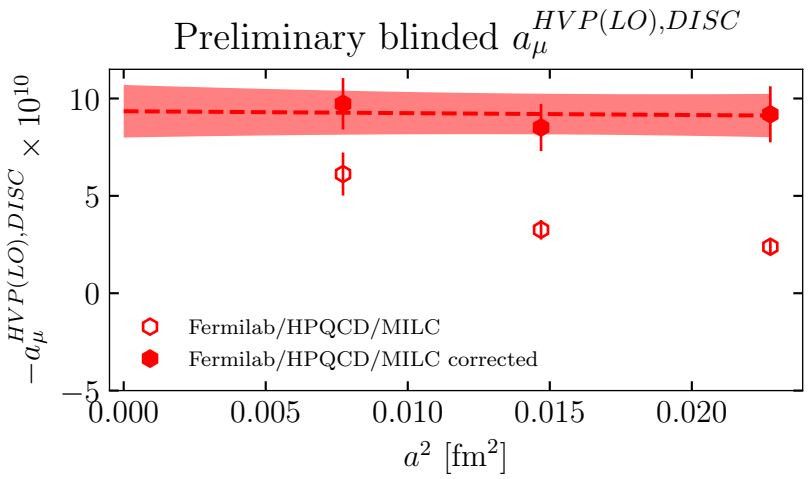

Figure 1: $a_\mu^{\mathrm{HVP(LO),DISC}}$ as a function of the square of the lattice spacing.

We use Bayesian fitting [31] with priors on the properties of ρ, excited ρ, ω and excited ω.

The raw data are corrected by including taste and finite volume corrections, using the model first developed in Ref. [7] and extended in Ref. [4]. Figure 1 shows the data and the data corrected for finite volume and taste corrections with the continuum extrapolation. $a_\mu^{\mathrm{HVP(LO),DISC}}$ is extrapolated to the continuum and physical pion masses using:

$$a_\mu^{\mathrm{HVP(LO),DISC}}(a, m_\pi) = a_0 \left(1 + a_1 (a\Lambda)^2 + a_2 \left(\frac{m_\pi^2 - m_{\pi,phys}^2}{m_{\pi,phys}^2}\right)\right) \tag{9}$$

where a is the lattice spacing in units GeV^{-1}, $\Lambda = 0.5$ GeV represents the QCD scale. Broad priors are included for the fit parameters: a_0, a_1, and a_2.

4. Preliminary window analysis of $a_\mu^{\mathrm{HVP(LO),DISC}}$

The lattice data can be with the experimental $e^+e^- \to$ hadrons scattering data [14, 32, 33]. It is useful to compare the $e^+e^- \to$ hadrons scattering data and lattice data for specific regions in time using a window function.

For the disconnected correlators there is currently no direct comparison between experimental data and the lattice correlator, but it is useful to compare the correlator at different time regions between lattice calculations, because this isolates different physics and parts of the correlator with different statistical properties. The following weight function in time is used [34, 35]

$$W(t; t_1, t_2) \equiv \Theta(t; t_1, \Delta) - \Theta(t; t_2, \Delta) \tag{10}$$

where

$$\Theta(t; t', \Delta) \equiv \frac{1}{2} + \frac{1}{2} \tanh\left[\frac{t - t'}{\Delta}\right] \tag{11}$$

and $\Delta = 0.15$ fm.

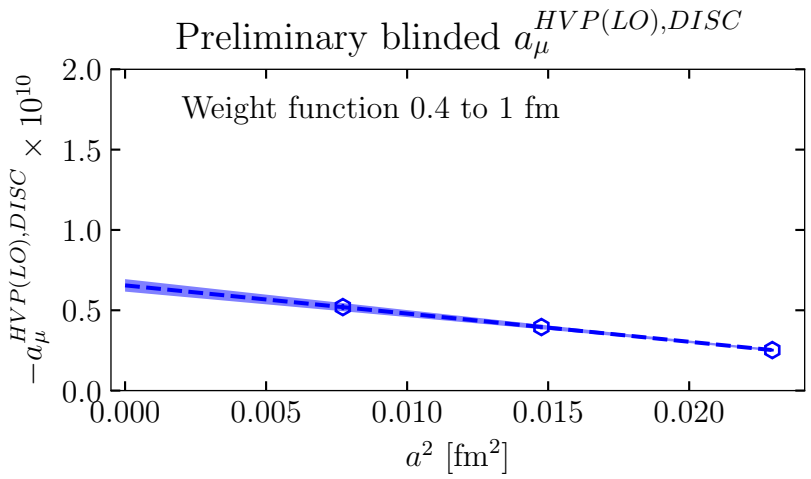

Figure 2: The weighted $a_\mu^{\mathrm{HVP(LO),DISC}}$(using the weight function in Eq. 10 with $t_1 = 0.4$ fm $t_2 = 1.0$ fm) as a function of the square of the lattice spacing.

Ensemble	a fm	m_π MeV	L fm	N_{meas}	Z_V^{QCD}	$Z_V^{\mathrm{QCD+QED}}$
Very coarse	0.15	134.7	4.8	356	0.95932(18)	0.999544(14)
Coarse (I)	0.12	132.7	5.8	300	0.97255(22)	0.999631(24)
Fine	0.09	128.3	5.8	128	0.98445(11)	0.999756(32)

Table 2: The gauge ensembles used to compute QCD + quenched QED correlators. The Z_V renormalization factors of the local current are from [19].

The weight function in Eq. 10 with parameters ($t_1 = 0.4$ fm $t_2 = 1.0$ fm) is applied to the blinded correlators. $a_\mu^{\mathrm{HVP(LO),DISC}}$is plotted in Fig. 2 using the specified weight function. No taste or finite volume corrections have been applied to the data in Fig. 2. RBC/UKQCD [34], and BMWc [35] also found a small contribution to $a_\mu^{\mathrm{HVP(LO),DISC}}$from this window.

5. Quenched QED corrections to the connected contribution to $a_\mu^{\mathrm{HVP,LO}}$

We present preliminary results for the connected QED contribution to the leading order hadronic contribution to $a_\mu^{\mathrm{HVP,LO}}$. We use the electro-quenched approximation [36–38] to partially include the dynamics of QED. The quenched QED fields were fixed to the Feynman gauge with zero modes dealt with using the QED$_L$ prescription [39].

Other collaborations estimate the QED contribution to QCD calculations by computing correlators in a perturbative expansion in the electric charge [40]. The RBC/UKQCD collaboration have compared the perturabtive QED approach to the electroqenched approach [41]. One potential advantage of the perturbative approach to including QED contributions is that there is a version of the formalism with the QED contribution in the infinite volume limit [42].

Table 2 lists the ensembles used in the analysis. The first physical coarse ensemble (I) generated by the MILC collaboration was used, rather than the coarse ensemble with the better tuned pion

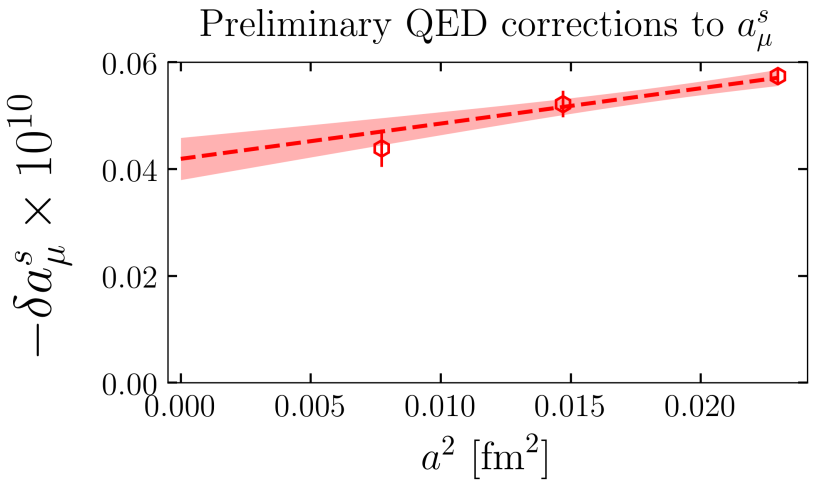

Figure 3: Strange quark contribution using lattice spacing and quark masses tuned against experiment in QCD.

mass in Table 1, because this ensemble was used to study quenched QED on the properties of charmonium [38]. The quark masses were tuned using only QCD with the lattice spacing determined from the gradient flow parameter w_0 also determined only including the dynamics of QCD.

The truncated solver method [28], with sloppy inversions on 16 source times and a precise inversion on one time source per lattice, was used to compute the vector correlator. The local vector current was used with the Z_V renormalization factor determined using the RI-SMOM scheme [19] in both QCD and QCD+QED (see Table 2.)

We initially generated correlators at the physical pion mass on the very coarse ensemble. Unfortunately the results were are noisy with measurements on 380 lattices. So, following, BMWc [35] we switched to extrapolating from the heavier light quark masses: $3m_l$, $5m_l$ and $7m_l$ to the physical light quark mass (m_l).

There are various ways to measure the contribution of the quenched QED on the results, in this calculation we use the difference.

$$\delta a_\mu^s = a_\mu^s[\text{QCD} + \text{qQED}] - a_\mu^s[\text{QCD}] \tag{12}$$

We have no estimate of the finite volume corrections to δa_μ^s; we plan to quantify these in the future. This analysis used only neutral correlators, hence the finite volume corrections from the inclusion of quenched QED is expected to be much less than for charged correlators. For example, HPQCD [38] found negligible finite volume corrections for the quenched QED corrections to the mass and decay constants of the J/ψ and η_c mesons, and moments of the charmed neutral vector correlator. The analysis of Bijnens et al. [43] found that the finite size effects in the QED corrections to the hadronic vacuum polarization starts at $O(\frac{1}{L^3})$ where L is the spatial lattice size.

In Fig. 3 we plot the QED contribution to the strange quark contribution to the HVP δa_μ^s, as a function of the square of the lattice spacing. To compare our continuum limit result in Fig. 3 with

those reported by BMWc [35], ETM collaboration [44], and RBC/UKQCD [34], one must convert them to a common scheme, which we have not yet done.

6. Conclusions

We have presented a progress report on two calculations that aim to decrease the errors on $a_\mu^{\rm HVP,LO}$. We are increasing the statistics on the fine ensemble for the calculation of the disconnected diagrams. Also we are increasing the statistics for the valence quenched QED contribution and investigating the tuning of the light quark masses and lattice spacings with quenched QED and QCD.

Acknowledgments

This work used the Extreme Science and Engineering Discovery Environment (XSEDE), which is supported by National Science Foundation grant number ACI-1548562. Specifically, we uses Ranch and Stampede 2 at the Texas Advanced Computing Center (TACC), located at the University of Texas at Austin, through XSEDE grant TG-MCA93S002. This research used the Cori supercomputer at the National Energy Research Scientific Computing Center (NERSC), a U.S. Department of Energy Office of Science User Facility located at Lawrence Berkeley National Laboratory, operated under Contract No. DE-AC02-05CH11231. This work used the DiRAC Data Analytic system at the University of Cambridge, operated by the University of Cambridge High Performance Computing Service on behalf of the STFC DiRAC HPC Facility (www.dirac.ac.uk). This equipment was funded by BIS National E-infrastructure capital grant (ST/K001590/1), STFC capital grants ST/H008861/1 and ST/H00887X/1, and STFC DiRAC Operations grant ST/K00333X/1. DiRAC is part of the National E-Infrastructure. We are grateful to the Cambridge HPC support staff for assistance.

This material is based upon work supported by Science and Technology Facilities Council, the U.S. Department of Energy, Office of Science, Office of Nuclear Physics under grant DE-SC0015655 (A.X.K.), and DE-SC0010120 (S.G.); by the U.S. National Science Foundation under Grants No. PHY17-19626 and PHY20-13064 (C.D., A.V.); and DOE/NNSA Exascale Computing Project (17-SC-20-SC) (C.D, A.V., S.G., H.J.).

References

[1] Muon g-2, B. Abi *et al.*, Phys. Rev. Lett. **126**, 141801 (2021), arXiv:2104.03281.

[2] Muon g-2, G. W. Bennett *et al.*, Phys. Rev. D **73**, 072003 (2006), arXiv:hep-ex/0602035.

[3] T. Aoyama *et al.*, Phys. Rept. **887**, 1 (2020), arXiv:2006.04822.

[4] Fermilab Lattice, HPQCD, MILC, C. T. H. Davies *et al.*, Phys. Rev. D **101**, 034512 (2020), arXiv:1902.04223.

[5] HPQCD, B. Chakraborty *et al.*, Phys. Rev. D **89**, 114501 (2014), arXiv:1403.1778.

[6] B. Chakraborty *et al.*, Phys. Rev. D **93**, 074509 (2016), arXiv:1512.03270.

[7] B. Chakraborty *et al.*, Phys. Rev. D **96**, 034516 (2017), arXiv:1601.03071.

[8] Fermilab Lattice, HPQCD, MILC, B. Chakraborty *et al.*, Phys. Rev. Lett. **120**, 152001 (2018), arXiv:1710.11212.

[9] B. Chakraborty, C. T. H. Davies, J. Koponen, G. P. Lepage, and R. S. Van de Water, Phys. Rev. D **98**, 094503 (2018), arXiv:1806.08190.

[10] Y. Lin *et al.*, Phys. Rev. D **103**, 034501 (2021), arXiv:1911.12256.

[11] C. Hughes, Y. Lin, and A. S. Meyer, PoS **LATTICE2019**, 057 (2019), arXiv:1912.00028.

[12] S. Lahert *et al.*, Hadronic vacuum polarization of the muon on 2+1+1-flavor HISQ ensembles: an update, https://indi.to/9GDTd, [Talk at lattice 2021; Online; accessed 21-December-2021].

[13] T. Blum, Phys. Rev. Lett. **91**, 052001 (2003), arXiv:hep-lat/0212018.

[14] D. Bernecker and H. B. Meyer, Eur. Phys. J. A **47**, 148 (2011), arXiv:1107.4388.

[15] X. Feng *et al.*, Phys. Rev. D **88**, 034505 (2013), arXiv:1305.5878.

[16] HPQCD, UKQCD, E. Follana *et al.*, Phys. Rev. D **75**, 054502 (2007), arXiv:hep-lat/0610092.

[17] MILC, A. Bazavov *et al.*, Phys. Rev. D **82**, 074501 (2010), arXiv:1004.0342.

[18] MILC, A. Bazavov *et al.*, Phys. Rev. D **87**, 054505 (2013), arXiv:1212.4768.

[19] HPQCD, D. Hatton, C. T. H. Davies, G. P. Lepage, and A. T. Lytle, Phys. Rev. D **100**, 114513 (2019), arXiv:1909.00756.

[20] Fermilab Lattice, HPQCD, MILC, S. Yamamoto *et al.*, PoS **LATTICE2018**, 322 (2019), arXiv:1811.06058.

[21] Fermilab Lattice, HPQCD, MILC, C. E. DeTar *et al.*, PoS **LATTICE2019**, 070 (2019), arXiv:1912.04382.

[22] ETM, P. Boucaud *et al.*, Comput. Phys. Commun. **179**, 695 (2008), arXiv:0803.0224.

[23] ETM, K. Jansen, C. Michael, and C. Urbach, Eur. Phys. J. C **58**, 261 (2008), arXiv:0804.3871.

[24] ETM, C. McNeile, C. Michael, and C. Urbach, Phys. Lett. B **674**, 286 (2009), arXiv:0902.3897.

[25] A. Abdel-Rehim *et al.*, Phys. Rev. D **89**, 034501 (2014), arXiv:1310.6339.

[26] L. Giusti, T. Harris, A. Nada, and S. Schaefer, Eur. Phys. J. C **79**, 586 (2019), arXiv:1903.10447.

[27] J. R. Klein and A. Roodman, Ann. Rev. Nucl. Part. Sci. **55**, 141 (2005).

[28] G. S. Bali, S. Collins, and A. Schäfer, Comput. Phys. Commun. **181**, 1570 (2010), arXiv:0910.3970.

[29] C. Alexandrou, K. Hadjiyiannakou, G. Koutsou, A. O'Cais, and A. Strelchenko, Comput. Phys. Commun. **183**, 1215 (2012), arXiv:1108.2473.

[30] W. M. Wilcox, PoS **LATTICE2007**, 025 (2007), arXiv:0710.1813.

[31] G. P. Lepage *et al.*, Nucl. Phys. B Proc. Suppl. **106**, 12 (2002), arXiv:hep-lat/0110175.

[32] RBC, UKQCD, C. Lehner, EPJ Web Conf. **175**, 01024 (2018), arXiv:1710.06874.

[33] C. Lehner and A. S. Meyer, Phys. Rev. D **101**, 074515 (2020), arXiv:2003.04177.

[34] RBC, UKQCD, T. Blum *et al.*, Phys. Rev. Lett. **121**, 022003 (2018), arXiv:1801.07224.

[35] S. Borsanyi *et al.*, Nature **593**, 51 (2021), arXiv:2002.12347.

[36] A. Duncan, E. Eichten, and H. Thacker, Phys. Rev. Lett. **76**, 3894 (1996), arXiv:hep-lat/9602005.

[37] MILC, S. Basak *et al.*, Phys. Rev. D **99**, 034503 (2019), arXiv:1807.05556.

[38] HPQCD, D. Hatton *et al.*, Phys. Rev. D **102**, 054511 (2020), arXiv:2005.01845.

[39] M. Hayakawa and S. Uno, Prog. Theor. Phys. **120**, 413 (2008), arXiv:0804.2044.

[40] RM123, G. M. de Divitiis *et al.*, Phys. Rev. D **87**, 114505 (2013), arXiv:1303.4896.

[41] P. Boyle *et al.*, JHEP **09**, 153 (2017), arXiv:1706.05293.

[42] C. Lehner and T. Izubuchi, PoS **LATTICE2014**, 164 (2015), arXiv:1503.04395.

[43] J. Bijnens *et al.*, Phys. Rev. D **100**, 014508 (2019), arXiv:1903.10591.

[44] D. Giusti, V. Lubicz, G. Martinelli, F. Sanfilippo, and S. Simula, PoS **CD2018**, 063 (2019), arXiv:1909.01962.